

Hyperfine interactions of ^{111}Cd in CuGeO_3 studied by perturbed angular correlations

V. V. Krishnamurthy,* S. Habenicht, K.-P. Lieb, and M. Uhrmacher

II. Physikalisches Institut, Universität Göttingen, Bunsenstrasse 7/9, D-37073 Göttingen, Germany

K. Winzer

I. Physikalisches Institut, Universität Göttingen, Bunsenstrasse 9, D-37073 Göttingen, Germany

(Received 29 January 1997)

The electric quadrupole interaction of ^{111}Cd in poly- and single-crystalline CuGeO_3 has been measured in the temperature range from 4.2 to 556 K, using perturbed angular correlation spectroscopy. Two electric field gradients have been observed: a well-defined one having a quadrupole interaction frequency of $\nu_q = 407$ MHz and an asymmetry parameter of $\eta = 0.34$ at room temperature, and a broadly distributed one. Possible sites for the implanted ^{111}In probes are discussed on the basis of the point charge model and perturbed angular correlation (PAC) results in CuO and other binary and ternary oxides. No anomalous change of the hyperfine interaction parameters has been detected at the spin-Peierls transition temperature T_{SP} . We suggest that the absence of an anomaly at T_{SP} is caused by the doping of CuGeO_3 with the ^{111}Cd PAC impurity, which prevents lattice distortions and spin dimerization at the nearest-neighbor Cu sites in Cu-O-Cu chains. [S0163-1829(97)01626-3]

I. INTRODUCTION

In the recent past, low-dimensional quantum spin systems with antiferromagnetic interactions have attracted significant interest because of their ground-state properties such as high- T_c superconductivity in layered cuprates, the appearance of the Haldane gap in integer-spin Heisenberg antiferromagnetic chains, and spin-Peierls (SP) transitions in alternating Heisenberg chains with half-integer spins. The SP transition in an $S = 1/2$ one-dimensional Heisenberg antiferromagnet is a transition to a nonmagnetic spin-singlet ground state at a characteristic temperature T_{SP} , due to the spin and lattice dimerizations caused by spin-phonon interactions. Recently, Hase, Terasaki, and Uchinokura¹ have reported on the observation of a SP transition in an inorganic compound, the quasi-one-dimensional Cu^{2+} ($S = 1/2$) antiferromagnet CuGeO_3 . In the room-temperature phase, CuGeO_3 has an orthorhombic unit cell with the lattice constants $a = 4.795$ Å, $b = 8.466$ Å, and $c = 2.940$ Å and the space group $Pbmm$.^{2,3} This structure contains four equivalent sites: one Cu site, one Ge site, and the two O sites, O(1) and O(2); ten atoms (two formula units) are found per unit cell. Figure 1, taken from Ref. 3, schematically represents the CuGeO_3 crystal structure, which can be described by corner-sharing GeO_4 tetrahedra and edge-sharing, deformed CuO_6 octahedra as building blocks. Along the c axis, two adjacent Cu^{2+} ions, each in the center of a planar cross of four oxygen ions, are connected by two O^{2-} ions which mediate the superexchange interaction. Nevertheless, comparing this structure to high- T_c superconducting cuprates shows an important difference in the crystal structures: Whereas the cuprate structures are completely filled by the different types of anion polyhedra, there exist rather large open volumes in the case of CuGeO_3 .³

The SP transition in CuGeO_3 is characterized by (i) an exponential drop of the magnetic susceptibility below the phase transition temperature $T_{\text{SP}} = 14$ K and (ii) the

$\Delta T_{\text{SP}}/T_{\text{SP}} \propto - (H^2)$ type magnetic-field-dependent reduction of T_{SP} . This discovery has initiated several experiments to study the structural and electronic properties associated with the spin and lattice dimerizations at the SP transition in this compound.⁴⁻⁷ X-ray- and inelastic-neutron-scattering measurements showed that CuGeO_3 exhibits a second-order structural transition to a dimerized ground state at T_{SP} and confirmed that the SP transition is driven by the magnetic Cu^{2+} chains. The experimental evidence of the expected spin dimerization has been reported by Pouget *et al.*⁴ on the basis of x-ray-diffraction analysis, and verified by Kamimura *et al.*⁵ by electron diffraction, through the observation of superlattice reflections with indices $h/2, k, l/2$ (h, k, l ; all odd) below T_{SP} . In neutron-diffraction experiments, Hirota *et al.* found additional superlattice reflections at indices $h/2, k, l/2$ (h, k, l ; k even).⁶ These authors proposed a structural model for the dimerized phase which is characterized by dimerized Cu^{2+} - Cu^{2+} pairs along the c axis, accompanied by alternating inward and outward displacements of the two O^{2-} ions in the Cu-O(2)-Cu chains along the c axis. In the dimerized phase, the doubled unit cell of CuGeO_3 at 4.2 K is described

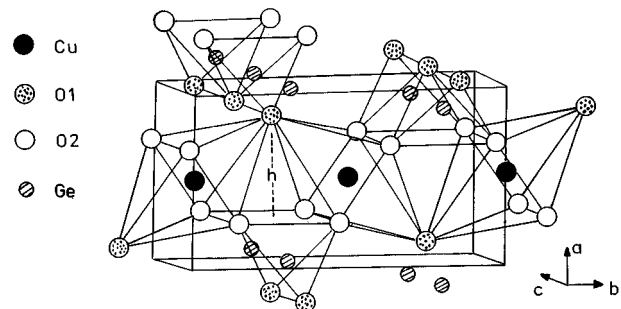


FIG. 1. Room-temperature crystal structure of CuGeO_3 taken from Ref. 3.

by the lattice constants $a=2\times 4.7894$ Å, $b=8.4018$ Å, and $c=2\times 2.9445$ Å with $Bbcm$ as the space group.³ Now one finds two equivalent Cu sites Cu_a and Cu_b .

While the SP transition in CuGeO_3 has been established unambiguously, some other questions still remain open, e.g., the suppression of three-dimensional antiferromagnetic ordering, the nature of the second-order structural transition to the dimerized state at T_{SP} , the structure of CuGeO_3 in the dimerized phase, and the coexistence of the SP transition with long-range antiferromagnetism in doped CuGeO_3 samples. In particular, the electric field gradient (EFG) at cation sites is sensitive to the electronic structure of the microsurrounding of the site and is expected to give information about the structural transition at T_{SP} and the dimerized phase. The EFG at the Cu site across the SP transition in CuGeO_3 has been previously investigated by Itoh, Hirashima, and Motaya⁸ using $^{63,65}\text{Cu}$ nuclear quadrupole resonance (NQR) measurements. In their study, the quadrupole-coupling constant ν_q , which was determined from the measured frequency $\nu_{\text{NQR}}=\nu_q\sqrt{1+\eta^2/3}$ by assuming the temperature-independent asymmetry parameter $\eta=0.16$, did not yield any noticeable change of the EFG at the Cu site across the SP transition. This result might be surprising at first glance, since the EFG tensor at the Cu site is strongly correlated with the Cu-O bond distances and the O-Cu-O bond angles, both changing abruptly at the SP transition. Nevertheless, the absolute changes in the positions are very small. Point charge model (PCM) calculations, already done by Itoh *et al.*⁸ predicted a negligible change of η between 0.8396 and 0.8394 across the SP transition. Our own PCM calculation predicts a change from 0.8805 to 0.8874. Such tiny changes, based only on the small structural change at the SP transition, cannot be observed by NQR or perturbed angular correlation (PAC). The predicted values, however, are in strong conflict with the value $\eta=0.16$ given in the same paper.

In the present study, we have investigated the structural and electronic properties of CuGeO_3 in the normal state and in the spin-Peierls state by measuring the hyperfine interactions at $^{111}\text{In}(\text{EC})^{111}\text{Cd}$ probes in CuGeO_3 , using the perturbed angular correlation method. The $I^\pi=5/2$ isomeric state of the ^{111}Cd nuclei, having a higher (by a factor of 4) spectroscopic quadrupole moment of $Q=0.83$ b, as compared to $Q=-0.209$ b of ^{63}Cu , is expected to sensitively probe the quadrupole interaction frequency ν_q and the asymmetry parameter η . In PAC measurements the temperature dependence and the asymmetry η of the EFG of the site can be measured without any *a priori* assumption on their relationship. Furthermore, the implanted probes are well suited to detect supertransferred hyperfine (HF) fields in antiferromagnets.^{9–11}

II. EXPERIMENTAL PROCEDURE

Polycrystalline samples of CuGeO_3 were prepared from a stoichiometric mixture of CuO and GeO_2 powders by a solid-state reaction in air at 1273 K for 3 h. The room-temperature crystal structure of the samples was determined by powder x-ray-diffraction measurements with the $\text{Cu } K_\alpha$ radiation. All the peaks could be identified with the known peaks of CuGeO_3 , and the lattice constants were found to be

in good agreement with the values reported in the literature.^{2,3} Pellets of CuGeO_3 , needed for the implantation of radioactive ^{111}In ions, were prepared by pressing the powder samples at 0.5 kbar. Single crystals of CuGeO_3 were grown from a 1:1.2 mixture of CuO and GeO_2 in a Pt crucible by the slow-cooling technique described in Ref. 12. In the present PAC measurements we used CuGeO_3 single crystals grown from the same batch which Liu *et al.* used in their specific-heat measurements.¹²

A dose of $\sim 10^{12}$ radioactive $^{111}\text{In}^+$ ions was implanted into the pellets or the single crystals at an implantation energy of 400 keV using the Göttingen ion implanter IONAS.¹³ In order to remove the implantation-induced lattice damage the polycrystalline CuGeO_3 samples were annealed in air at 1273 K for 3 h and the single-crystal samples at 1173 K for 4 h. The ^{111}In radioactive nuclei decay via electron capture, with a half-life of 2.83 days, to the 416 keV excited state of ^{111}Cd . The hyperfine interaction occurs between the nuclear moments of ^{111}Cd in the 245 keV, $I^\pi=5/2^+$ isomeric state (having a mean life of $\tau=122$ ns, a quadrupole moment of $Q=0.83$ b, and a nuclear g factor of $g=0.74$), and the electromagnetic hyperfine fields present in the host lattice. The hyperfine interaction was detected by measuring the time modulations of the γ - γ angular correlation function $W(\theta, t)$ of the 171–245 keV cascade. A detailed description of the principles of PAC can be found in Refs. 14 and 15.

In the present study, we measured the time-differential perturbed angular correlation functions $N(\theta, t)$ in a conventional slow-fast or fast-fast coincidence setup with four $\text{NaI}(\text{Tl})$ or BaF_2 detectors, arranged in the standard 90° - 180° geometry. After annealing the samples, the PAC measurements were carried out at 4.2 K (in a liquid He bath), at 8–300 K (in a closed-cycle He cryostat), and at 300–560 K (in a vacuum oven). These experimental arrangements have been described previously.^{16,17}

In the case of polycrystalline samples, the perturbation functions

$$R(t) = 2 \frac{N(180, t) - N(90, t)}{N(180, t) + 2N(90, t)} \quad (1)$$

were generated from the measured coincidence yields $N(\theta, t)$ and fitted with the perturbation function relating to static electric quadrupole interactions,

$$R(t) = A_{22} \sum_i f_i G_{22}^i(t), \quad (2)$$

where the expression

$$G_{22}^i(t) = \sum_{n=0}^3 S_{2n}(\eta_i) \cos[g_{2n}(\eta_i) \nu_{qi} t] \times \exp[-g_{2n}(\eta_i) \delta_i t] d[g_{2n}(\eta_i) \nu_{qi} t, \tau_R] \quad (3)$$

refers to the EFG_{*i*} in polycrystalline samples. Here $S_{2n}(\eta)$ denotes the amplitudes of the primary transition frequencies¹⁸ $\omega_n = g_{2n}(\eta) \nu_q$, while the function $d[g_{2n}(\eta) \nu_{qi} t, \tau_R]$ accounts for the damping of $G_{22}^i(t)$ due to the finite time resolution of the apparatus. The quadrupole-coupling constant $\nu_{qi} = eQV_{zz}^{(i)}/h$ measures the largest component $V_{zz}^{(i)}$ of the *i*th EFG tensor, and its symmetry is given by the

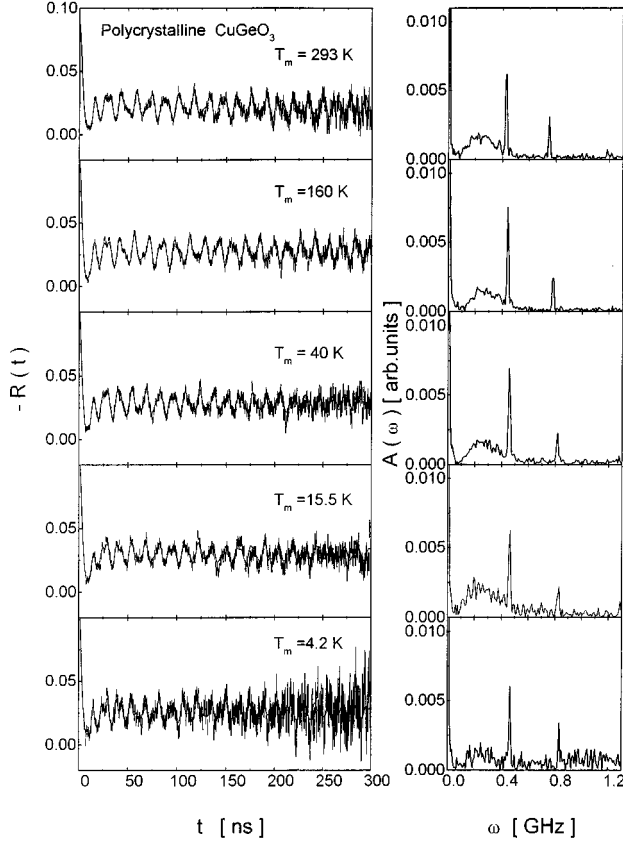


FIG. 2. Spin rotation spectra and their Fourier transforms showing the electric quadrupole interaction of ^{111}Cd in polycrystalline CuGeO_3 at different measuring temperatures.

asymmetry parameter $\eta_i = (V_{xx}^{(i)} - V_{yy}^{(i)}) / V_{zz}^{(i)}$ where $0 \leq \eta_i \leq 1$. The components V_{ij} of the EFG tensor are arranged in such a way that $|V_{xx}| \leq |V_{yy}| \leq |V_{zz}|$. The quantity A_{22} is the effective anisotropy of the γ - γ cascade and δ_i denotes the width of the Gaussian-type distribution of the quadrupole frequencies. When more than one hyperfine-interaction site contributes to the PAC signal, the relative fractions i are labeled f_i .

III. RESULTS

A. Polycrystalline samples

Figure 2 shows some measured perturbation functions $R(t)$ with their fits and Fourier transforms, taken for polycrystalline samples of CuGeO_3 at measuring temperatures T_m in the range of 4.2–556 K. All the spectra are characterized by fast oscillations associated with an EFG at the ^{111}Cd site. The Fourier transforms show two distinct features: first, a set of two sharp peaks, which are identified as the components ω_1 and ω_2 , in the higher-frequency regime with an almost-temperature-independent width of $\delta \sim 2$ MHz, corresponding to an asymmetric ($\eta \neq 0$) EFG (henceforth referred to as EFG₁). The Fourier component ω_3 of EFG₁ is barely visible in the Fourier spectra taken with NaI detectors due to the large damping caused by the finite time resolution. For demonstration, one Fourier spectrum taken with BaF_2 detectors and the single crystal is given in Fig. 4(a).

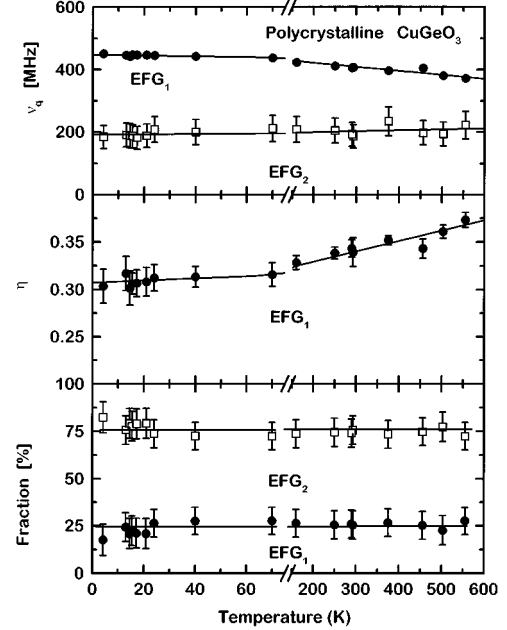


FIG. 3. Temperature dependence of the quadrupole frequencies ν_q , asymmetry parameter η , and fractions f_1 and f_2 measured in polycrystalline samples. The lines are given to guide the eye. The fractions f_1 and f_2 add up to 100%.

The second feature of all Fourier spectra is a broad bump centered at a lower frequency, typical of a broad distribution of EFG's (denoted as EFG₂). For broadly distributed EFG's, the distribution parameters ν_q and η cannot be determined independently of each other. As shown by Forker¹⁹ in the case of a distribution width of $\delta \geq 30\%$, it is appropriate to fix η to 0.5 and fit the centroid and width of the ν_q distribution, as has been done in the present case. Fits were found to improve when EFG₂ was fitted with a Lorentzian distribution.

Figure 2 also shows that the quadrupole parameters smoothly change as a function of the measuring temperature T_m . A summary of the temperature dependence of the two quadrupole frequencies ν_{q1} and ν_{q2} , of the asymmetry parameter η_1 and the two fractions f_1 and f_2 is given in Fig. 3. Apart from a slight decrease of ν_{q1} and increase of η_1 with T_m , we did not observe any significant change of the EFG parameters. In particular, there did not occur any measurable change of the sharp EFG₁ across the SP transition at 14 K. For a detailed comparison of EFG parameters, see Table I.

B. Single-crystal measurements

In PAC measurements with single crystals the spectra sensitively depend on the relative orientation of the crystal with respect to the detector geometry.^{14,20,21} Under favorite conditions this allows us to determine the directions of the EFG tensor components V_{ij} in the crystal lattice. In the present case we used the single crystals from a batch for which Liu *et al.* had observed the SP transition,¹² in order to countercheck our pressed-powder samples. The closed-cycle He cryostat allowed only a rotation of the sample in the detector plane for the price of different γ absorption in the four detectors. Therefore, we have chosen an orientation of

TABLE I. Summary of the measured EFG parameters ν_{qi} (MHz), η_i , and f_i (%) for ^{111}Cd in poly- and single-crystalline CuGeO_3 at different measuring temperatures T_m .

System	T_m (K)	i	ν_{qi} (MHz)	η_i	f_i (%)
CuGeO_3 (polycrystalline)	556	1	372(3)	0.37(1)	28(7)
		2	222(44)	0.5(fixed)	72(7)
	293	1	407(4)	0.34(1)	25(7)
		2	186(37)		75(7)
	17.2	1	447(6)	0.31(1)	21(8)
		2	208(41)		79(8)
	4.2	1	450(4)	0.30(2)	18(8)
		2	184(36)		82(8)
CuGeO_3 (single crystal)	293	1	408(7)	0.34(1)	32(7)
		2	326(3)	0.5(fixed)	68(7)
	83	1	435(6)	0.32(1)	27(7)
		2	216(22)		73(7)
	17	1	447(6)	0.31(2)	38(6)
		2	244(24)		62(6)
	8.3	1	452(7)	0.30(2)	44(6)
		2	275(28)		56(6)
CuO (polycrystalline)	293	1	420(1)	0.42(1)	≤ 50
		2	147(40)	0.8	

the c axis pointing towards one of the detectors, kept the 90° - 180° detector geometry, and rotated the cold target holder in order to achieve high amplitudes for the primary transition frequencies ω_1 and ω_2 . As the frequency factors $g_{2n}(\eta) = \omega_n/\nu_q$ only depend on the asymmetry parameter η , but not on the crystal-axis orientation relative to the detectors, the experimental value $\omega_2/\omega_1 = g_{22}/g_{21}$ can be used to determine η with the high precision. This seemed to be important in the context of the spin-Peierls transition in CuGeO_3 . Several perturbation functions and their Fourier transforms obtained for the quadrupole interaction of ^{111}Cd in CuGeO_3 single-crystal samples at various measuring temperatures T_m are displayed in Fig. 4. The perturbation functions observed in the finally chosen geometry were very similar to those obtained in polycrystalline samples. Hence, the corresponding $R(t)$ spectra measured with the single-crystal samples were fitted by the expression defined in Eq. (2). Again we found the well-defined EFG₁ and the broadly distributed EFG₂. The single-crystal measurements again did not show any measurable changes of ν_{q1} and η_1 across the SP transition. As indicated in Fig. 5 and Table I, the EFG parameters for the single crystals show the same temperature dependence as in the polycrystalline samples and, indeed, are in very good agreement with each other. The only difference relates to the fraction f_1 of the well-defined EFG₁, which is slightly higher in the single crystal.

IV. DISCUSSION

The most evident result of our experiments is the absence of any sudden changes in the quadrupole interaction over the whole temperature range, especially across the SP transition in CuGeO_3 . Different to the case of the NQR experiment, we first have to discuss the possible site(s) of the $^{111}\text{In}/^{111}\text{Cd}$ probe atoms which are impurities. After introducing the

point charge model we will discuss various sites for the PAC probe ^{111}In in the CuGeO_3 structure and compare the measured EFG₁ with that in other oxides, with PCM predictions and with the results of ^{63}Cu -NQR. Finally assuming that ^{111}In substitutes Cu, we shall discuss the observed absence of any anomaly in the PAC parameters.

A. Point charge model

The simplest method to calculate an EFG in ionic compounds is the point charge model (PCM) where appropriate point charges are attached at the atomic positions. In fact, EFG's in oxides can often be well predicted by the PCM.²² The lattice contribution to the EFG at a ^{111}Cd impurity, occupying a Cu or a Ge site in the CuGeO_3 lattice was calculated by assuming the formal charges q_n of Cu^{2+} , Ge^{4+} , and O^{2-} at their respective crystallographic locations. For a probe atom located at the origin, the EFG is given by

$$V_{zz}^{\text{latt}} = V_{ij} = \sum_n q_n \frac{3x_n^i x_n^j - \delta_{ij} \text{mod} x_n^2}{\text{mod} x_n^2}, \quad (4)$$

where the summation index n runs over all the ions in the crystal and q_n is the charge of the n th ion. In the present calculations the lattice sum runs over all the ions within a sphere of 50 \AA radius.

The largest (z) component of the total EFG tensor is given by

$$V_{zz}^{\text{tot}} = V_{zz}^{\text{latt}}(1 - \gamma_\infty), \quad (5)$$

where the Sternheimer antishielding factor $\gamma_\infty = -29.27$ is the value appropriate for ^{111}Cd .²³ The calculated PCM parameters for the different sites in CuGeO_3 at different temperatures are given in Table II. PCM calculations and PAC measurements of EFG's at Cd impurities in binary and ter-

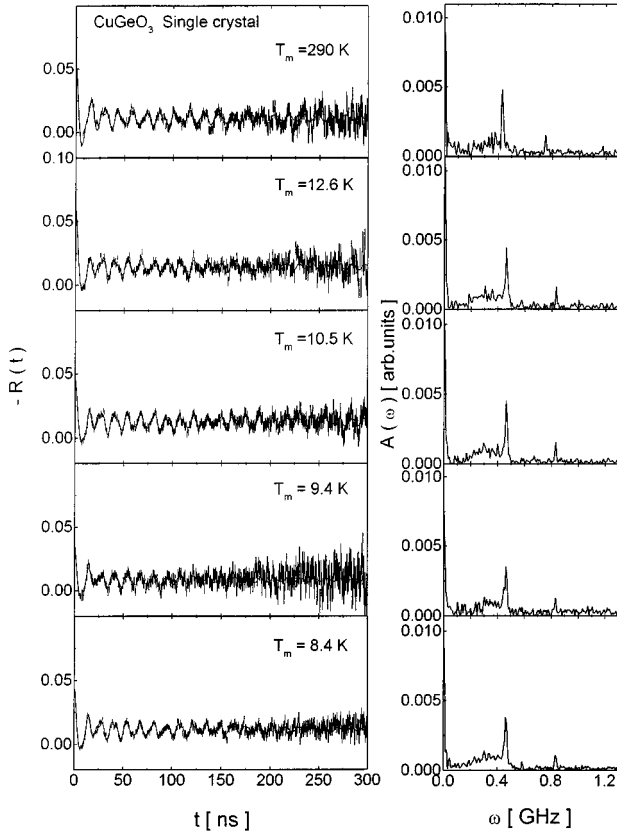


FIG. 4. Spin rotation spectra and their Fourier transforms showing the electric quadrupole interaction of ^{111}Cd in a CuGeO_3 single crystal at different measuring temperatures.

nary oxides have been compiled by Wiarda *et al.*²² and Attili *et al.*¹⁷ There it has been shown that the PCM gives reliable predictions of the strength and asymmetry of the EFG if the cation-oxygen bond length exceeds 2.1 Å. At shorter distances the atomic shells of probe and neighbor atoms overlap and one observes either an increase of the Sternheimer factor up to 90 or a decrease down to 8–10 (as in CuO).²² Another finding was that the power of PCM in predicting the strength of an EFG is still debatable, although the PCM generally reproduces the asymmetry parameter η quite well.

B. Cu site

Implantation of radioactive ^{111}In tracer ions into oxides and subsequent annealing of the induced damage usually

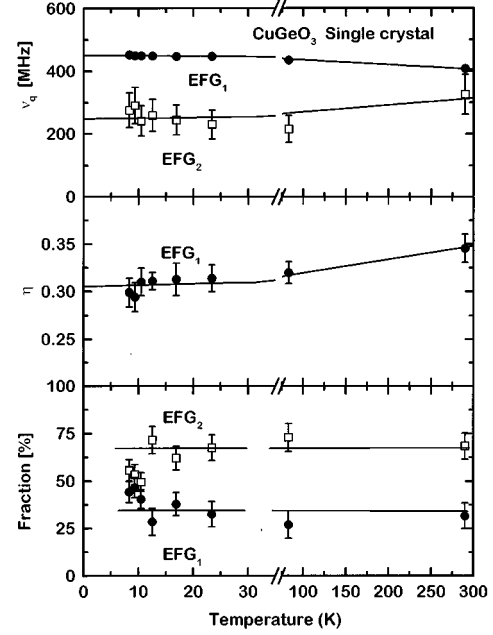


FIG. 5. Temperature dependence of the ^{111}Cd electric quadrupole interaction parameters ν_q (a), η (b), and fractions f_i of the two EFG's in a single-crystal CuGeO_3 sample (c). The lines are given to guide the eye. The fractions f_1 and f_2 add up to 100%.

leaves the probes on substitutional cation sites. As described by Lupascu *et al.*²⁴ two major origins of a nonstoichiometric occupation of cation sites must be considered: (1) The size of the probe ion does not fit well into the lattice. (2) In compounds with sites of different valency the stable $^{111}\text{In}^{3+}$ ion occupies a site with valency 3+. In the present case of CuGeO_3 there are only Cu^{2+} and Ge^{4+} cationic sites. In previous PAC experiments in binary and ternary oxides after ^{111}In -ion implantation,²² in most cases $^{111}\text{In}^{3+}$ was found to favor the sixfold oxygen coordination of an octahedral next neighborhood. Such an oxygen octahedron encloses the Cu site in CuGeO_3 . The Cu-O distance in the basal plane of the octahedron [$d(\text{Cu-O})=1.94$ Å] is short compared to the distance of the other two oxygen ions on the tips of the octahedron [$d(\text{Cu-O})=2.76$ Å], a situation quite similar to the case of CuO with its 2+ valent Cu site. In fact, the EFG parameters of ^{111}Cd in CuO [$\nu_q=420$ MHz, $\eta=0.42$ (Ref. 25)] are close to the ones observed here in CuGeO_3 . In CuO , too, a broad EFG₂ distribution appeared (see Table I). To detect

TABLE II. Results of PCM calculations for different sites in CuGeO_3 . Given are the frequency ν_q (MHz) and η at three different temperatures.

Site	293 K		20 K		4.2 K	
	ν_q (MHz)	η	ν_q (MHz)	η	ν_q (MHz)	η
Cu	541	0.872	539	0.888	537	0.881
Ge	300	0.372	297	0.366	293	0.361
Interstitial	407	0.39 0.50	447	0.42 0.51	450	0.28 0.52
Experimental	407(4)	0.34(1)	447(6)	0.31(1)	450(4)	0.30(2)

the presence of any CuO in the samples, we carefully measured the PAC spectra in the region around the Néel temperature $T_N(\text{CuO}) = 230$ K, but did not find any indication of a splitting of the Fourier peaks due to the antiferromagnetic ordering, as previously observed in CuO.⁹

If one assumes that ^{111}In occupies the Cu site in CuGeO_3 , the lattice contribution of EFG₁, V_{zz}^{latt} , found in the PAC experiment should be the same as that found with ^{63}Cu NQR. The lattice contribution V_{zz}^{latt} can be estimated using the relation $V_{zz}^{\text{latt}} = V_{zz}^{\text{tot}} / (1 - \gamma_\infty)$. From our PAC measurement, $\nu_{q1} = 450(4)$ MHz at $T_m = 4.2$ K, and using the value of $\gamma_\infty = -29.27$ for Cd,²³ we obtain the lattice part $V_{zz}^{\text{latt}} = 7.4 \times 10^{20}$ V/m². The measured ^{63}Cu NQR frequency in CuGeO_3 at $T_m = 4.2$ K in zero external field is $^{63}\nu_q = 33.95(11)$ MHz.⁸ Using the quadrupole moment $Q(^{63}\text{Cu}) = -0.209$ b and the Sternheimer antishielding factor $\gamma_\infty = -17.37$ for ^{63}Cu ,²³ we arrive at $V_{zz}^{\text{latt}} = 3.7 \times 10^{20}$ V/m², which is half the value obtained for ^{111}Cd .

As already mentioned above there is another serious problem with the assumption of ^{111}In probes residing at the Cu site. The asymmetry parameter η calculated in the PCM varies between 0.84 and 0.89 and clearly differs from the PAC measurement ($\eta = 0.34 - 0.37$) and from the NQR experiment ($\eta = 0.16$). In comparing the geometries of the octahedra in CuO and in CuGeO_3 around Cu which primarily determine η , there is a planar basal plane made by four oxygen ions. In CuO they span a perfect square ($a = b$), whereas in CuGeO_3 one finds $a = 2.9$ Å and $b = 2.5$ Å. This distortion produces the high η value. As the PCM predictions of η are in most cases reliable, the small experimental value argues against the location of $^{111}\text{In}/^{111}\text{Cd}$ on the Cu site.

C. Ge site

The second possible cation site for ^{111}In in CuGeO_3 would be the Ge site in the center of an oxygen tetrahedron. Up to now, only one example is known in oxides [Mn_3O_4 (Ref. 26)], where ^{111}In replaced the central cation of a tetrahedron. In $\beta\text{-Ga}_2\text{O}_3$, where octahedra and tetrahedra are the building blocks of the structure, ^{111}In ions only replace the cation in the octahedron.²⁷ Checking the empirical rules of Ref. 24, an additional argument against the Ge site comes from the short distance $d(\text{Ge-O}) = 1.74$ Å, which is far below the critical distance of about 2.1 Å corresponding to the sum of the ionic radii of a Cd^{2+} and an O^{2-} .²² In fact, the tetrahedron is nearly perfect and shows mainly covalent bonding³ which cannot be described by the PCM. On the other hand, the PCM calculation for the probe on the Ge site would reproduce the experimental η value ($\eta = 0.37$ at room temperature). Therefore we cannot definitely rule out an occupation of the Ge site.

D. Interstitial site

It was mentioned by Braden *et al.*³ that the CuGeO_3 structure contains rather large empty cavities. Inspection of Fig. 1 shows large empty pyramids between the Cu site octahedra. The basal plane of such a pyramid is made of four O(2) ions, on the top of which sits an O(1) ion. PCM calculations were performed placing the ^{111}Cd probe along the central axis at different heights h . The variations of ν_q and

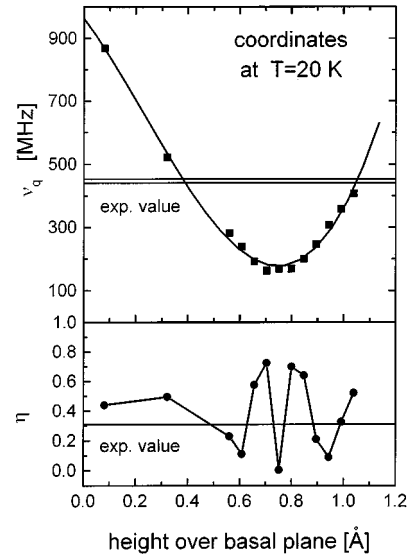


FIG. 6. Dependence of the ^{111}Cd electric quadrupole interaction parameters ν_q and η_1 on the interstitial position h along the axis of the empty pyramid.

η along this axis h are plotted in Fig. 6 for $T = 20$ K. The horizontal lines indicate the experimental data for EFG₁. Agreement in ν_q and η between the PCM calculation and the data is found for two positions of the probe: either close to $h = 0.4$ Å or $h = 1.05$ Å above the basal plane. Fixing ν_q to the experimental value we find better agreement in η for the lower value $h = 0.4$. A second argument for such an interstitial site can be extracted from the measured temperature dependence of ν_{q1} which increases when the temperature is lowered. CuGeO_3 has a pronounced anisotropy in its thermal-expansion parameters. Although there is a significant volume reduction, almost all cation-anion distances increase on cooling.³ As a consequence, the EFG on a cation site should decrease, as can be verified from the PCM results in Table II. On the other hand, lowering the temperature reduces the free space in CuGeO_3 and consequently the distance of the probe ion on the interstitial site to its next neighbors; therefore, the EFG increases, in agreement with the data. However, the calculated temperature dependence of η is not in agreement with the data.

E. Spin-Peierls phase transition

In view of the different arguments concerning the site allocation presented in the preceding sections we cannot arrive at a definite conclusion on the site of the radioactive ^{111}In probes in CuGeO_3 . The main reason why we favor the Cu site in CuGeO_3 is the close similarity of the EFG parameters to that in CuO which, in fact, is a precursor compound in the chemical synthesis of CuGeO_3 . In CuO the ^{111}Cd probes rest on the Cu site and sense, via combined hyperfine interactions, the antiferromagnetic ordering below T_N .^{25,9} But looking at the PCM calculations summarized in Table II, it is clear that the EFG₁ parameters do not show a measurable change at the SP transition temperature, in agreement with the NQR measurements. As the last step in the discussion we propose another possible explanation why no anomaly was observed in our PAC experiments at the SP transition. This transition is associated with the displace-

ments of Cu^{2+} and O^{2-} ions in the Cu-O(2)-Cu chains running along the c axis, where two adjacent Cu^{2+} ions ($S=1/2$) along the c axis undergo spin dimerization to form a spin-singlet (nonmagnetic) ground state. The substitution of the nonmagnetic Cd^{2+} ($S=0$) impurity for the Cu^{2+} ($S=1/2$) ion and the resulting slight rearrangement of Cd-O bonds or O-Cd-O angles may not be ideally suited for spin-Peierls-type lattice distortion and Cu-Cu spin dimerization next to Cd ions. The possible reason for not observing an anomaly in the measured quadrupole interaction parameters at $T_m \sim T_{\text{SP}}$ could be that the first- and second-nearest-neighbor Cu ions of Cd in the Cu-O(2)-Cu chains do not form spin dimers below $T_{\text{SP}}=14$ K and the lattice distortion is also prevented at these Cu ions. Our results for an extremely dilute Cd impurity in CuGeO_3 support the assumption of a reduced lattice distortion at a non-magnetic impurity, used by Fukuyama *et al.*²⁸ in their theoretical calculations, which correctly reproduce the experimentally observed coexistence of antiferromagnetic order with a spin-Peierls transition in Zn- or Si-doped CuGeO_3 samples.^{29,30}

V. SUMMARY

In summary, we have investigated the electric quadrupole interaction of ^{111}Cd in polycrystalline and single-crystal samples of the spin-Peierls compound CuGeO_3 in the tem-

perature range 4.2–556 K using PAC. A well-defined electric field gradient (EFG_1) and a broad EFG distribution (EFG_2) have been detected. The EFG having the quadrupole parameters $\nu_{q1}=407(4)$ MHz and $\eta_1=0.34(1)$ at room temperature has been tentatively attributed to ^{111}Cd replacing the Cu sites although the PCM does not support this claim. On the other hand, the results of the NQR experiments can be regarded as an indication for a smaller η than predicted by the PCM. No anomaly is detected in the hyperfine interaction parameters at the spin-Peierls transition temperature $T_{\text{SP}}=14$ K. We suggest that the smooth variation of ν_{q1} and η_1 at T_{SP} is caused by the doping of Cu in CuGeO_3 by nonmagnetic $\text{Cd}(S=0)$; i.e., the spin-Peierls-type lattice distortion and spin dimerization do not occur locally at the Cu ions adjacent to Cd impurities along the c axis in Cu-O(2)-Cu chains.

ACKNOWLEDGMENTS

The authors would like to thank Professor H. von Löhneisen and Dr. R. K. Kremer for kindly providing the single crystals of CuGeO_3 , Dr. L. Ziegeler for his help during the preparation of the polycrystalline samples, and Dr. M. Hase for very helpful discussions. This work is supported by the Deutsche Forschungsgemeinschaft.

*Present address: Muon Science Laboratory, The Institute for Physical and Chemical Research (RIKEN), Wako, Saitama 351-01, Japan.

¹M. Hase, I. Terasaki, and K. Uchinokura, *Phys. Rev. Lett.* **70**, 3651 (1993).

²H. Vollenkle, A. Wittmann, and H. Nowotny, *Monatsch. Chem.* **98**, 1352 (1967).

³M. Braden, G. Wilkendorf, J. Lorenzana, M. Ain, G. J. McIntyre, M. Behruzi, G. Heger, G. Dhalenna, and A. Revcolevschi, *Phys. Rev. B* **54**, 1105 (1996).

⁴J. P. Pouget, L. P. Regnault, M. Aim, B. Hennion, J. P. Renard, P. Veillet, G. Dhalenne, and A. Revcolevschi, *Phys. Rev. Lett.* **72**, 4037 (1994).

⁵O. Kamimura, M. Terauchi, M. Tanaka, O. Fujita, and J. Akimitsu, *J. Phys. Soc. Jpn.* **63**, 2870 (1994).

⁶K. Hirota, D. E. Cox, J. E. Lorenzo, G. Shirane, J. M. Tranquada, M. Hase, K. Uchinokura, H. Kojima, Y. Shibuya, and I. Tanaka, *Phys. Rev. Lett.* **73**, 736 (1994).

⁷T. M. Brill, J. P. Boucher, J. Vairon, G. Dhalenne, A. Revcolevschi, and J. P. Renard, *Phys. Rev. Lett.* **73**, 1545 (1994).

⁸M. Itoh, S. Hirashima, and K. Motaya, *Phys. Rev. B* **52**, 3410 (1995).

⁹A. Bartos, M. Uhrmacher, K. P. Lieb, and W. Bolse, *Hyperfine Interact.* **50**, 619 (1989).

¹⁰Th. Wenzel, M. Uhrmacher, and K. P. Lieb, *J. Phys. Chem. Solids* **55**, 684 (1994).

¹¹M. Uhrmacher, R. N. Attili, K. P. Lieb, K. Winzer, and M. Mekata, *Phys. Rev. Lett.* **76**, 4829 (1996).

¹²X. Liu, J. Wosnitza, H. v. Löhneysen, and R. K. Kremer, *Z. Phys. B* **98**, 163 (1995).

¹³M. Uhrmacher, K. Pampus, F. J. Bergmeister, D. Purschke, and

K. P. Lieb, *Nucl. Instrum. Methods Phys. Res. B* **9**, 234 (1985).

¹⁴H. Frauenfelder and R. M. Steffen, in *Alpha-, Beta-, and Gamma-Ray Spectroscopy*, edited by K. Siegbahn (North-Holland, Amsterdam, 1965).

¹⁵G. Schatz and A. Weidinger, *Nukleare Festkörperphysik* (Teubner, Stuttgart, 1992).

¹⁶A. Bartos, K. Schemmerling, Th. Wenzel, and M. Uhrmacher, *Nucl. Instrum. Methods Phys. Res. A* **330**, 132 (1993).

¹⁷R. N. Attili, M. Uhrmacher, K. P. Lieb, L. Ziegler, M. Mekata, and E. Schwarzmann, *Phys. Rev. B* **53**, 600 (1996).

¹⁸J. Kajfosz (unpublished).

¹⁹M. Forker, *Nucl. Instrum. Methods* **106**, 121 (1973).

²⁰D. Wegner, *Hyperfine Interact.* **23**, 179 (1985).

²¹D. Lupascu, A. Bartos, K. P. Lieb, and M. Uhrmacher, *Z. Phys. B* **93**, 441 (1994).

²²D. Wiarda, M. Uhrmacher, A. Bartos, and K. P. Lieb, *J. Phys. Condens. Matter* **5**, 4111 (1993).

²³F. D. Feiock and W. R. Johnson, *Phys. Rev.* **187**, 39 (1969).

²⁴D. Lupascu, M. Neubauer, T. Wenzel, M. Uhrmacher, and K. P. Lieb, *Nucl. Instrum. Methods Phys. Res. B* **113**, 507 (1996).

²⁵A. Bartos, W. Bolse, K. P. Lieb, and M. Uhrmacher, *Phys. Lett. A* **130**, 177 (1988).

²⁶A. F. Pasquevich, M. Uhrmacher, L. Ziegeler, and K. P. Lieb, *Phys. Rev. B* **48**, 10 052 (1993).

²⁷D. Wiarda, T. Wenzel, M. Uhrmacher, and K. P. Lieb, *J. Phys. Chem. Solids* **53**, 1199 (1992).

²⁸H. Fukuyama, T. Tanimoto, and M. Saito, *J. Phys. Soc. Jpn.* **65**, 1182 (1996).

²⁹M. Hase, K. Uchinokura, R. J. Birgeneau, K. Hirota, and G. Shirane, *J. Phys. Soc. Jpn.* **65**, 1392 (1996).

³⁰J. P. Renard, K. LeDang, P. Veillet, G. Dhalenne, A. Revcolevschi, and L. P. Regnault, *Europhys. Lett.* **30**, 475 (1995).